CHEMISTRY OF MATERIALS

Article

pubs.acs.org/cm

Poly(benzodithiophene) Homopolymer for High-Performance Polymer Solar Cells with Open-Circuit Voltage of Near 1 V: A Superior Candidate To Substitute for Poly(3-hexylthiophene) as Wide Bandgap Polymer

Tae Eui Kang,[‡] Taesu Kim,[‡] Cheng Wang,[§] Seunghyup Yoo,[∥] and Bumjoon J. Kim*[,‡]

[‡]Department of Chemical and Biomolecular Engineering and [∥]Department of Electrical Engineering, Korea Advanced Institute of Science and Technology (KAIST), Daejeon 305-701, Republic of Korea

[§]Advanced Light Source, Lawrence Berkeley National Laboratory, Berkeley, California 94720, United States

Supporting Information

ABSTRACT: Conjugated homopolymers can be synthesized more simply and reproducibly at lower cost than widely developing donor−acceptor (D−A) alternating copolymers. However, except for well-known poly(3-hexylthiophene) (P3HT), almost no successful homopolymer-based polymer solar cells (PSCs) have been reported because of their relatively wide band gap and unoptimized energy levels that limit the values of short circuit current (J_{SC}) and open-circuit voltage (V_{OC}) in PSCs. Herein, we report the development of poly(4,8-bis(5-(2-ethylhexyl)thiophen-2-yl)benzo[1,2-b:4,5-b']dithiophene) (PBDTT) homopolymer that has high light absorption coefficients and nearly perfect energy alignment with that of [6,6]-phenyl-C_{71}-butyric acid methyl ester ($PC_{71}BM$). Therefore, we were able to produce high-performance PSCs with the power conversion efficiency (PCE) of 6.12%, benefiting from both high V_{OC} (0.93 V) and J_{SC} (11.95 mA cm^{-2}) values. To the best of our knowledge, this PCE value is one of the highest values reported for the homopolymer donor-based PSCs. Significantly, the optimized condition of the device was achieved without any solvent additive or thermal treatment. Therefore, PBDTT is a promising candidate to take over the role of P3HT in tandem solar cells and ternary blend solar cells.

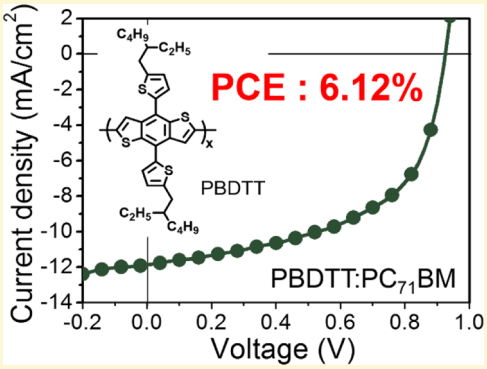

INTRODUCTION

The alternating push−pull type copolymers consisting of electron-rich (D) and electron-deficient (A) units in one polymer backbone (D−A alternating copolymers) have been extensively investigated in order to achieve better light harvesting and produce highly efficient polymer solar cells (PSCs).[1−8] However, although affordable price and time-cost for scale-up synthesis of conjugated polymers are essential for commercial application of PSCs, D−A alternating copolymers are not well-suited to this condition because of their multiple synthesis steps required to produce more than two different types of monomers.[9,10] In addition, for most D−A alternating copolymers, the process for optimizing their device performances typically requires the use of high-boiling-point additives, such as 1,8-diiodooctane (DIO) and 1-chloronaphthalene (CN), because of their relatively weak crystalline behavior and nonoptimized bulk-heterojunction (BHJ) morphology.[11−14] The use of these additives increases the cost of fabricating the devices and decreases the reliability of the devices because of the difficulty of removing the high-boiling point additives. Even the optimized devices often have poor stability (i.e., low thermal stability) because of residual solvent additives, which can cause severe phase separation of the BHJ morphology and poor reproducibility.[15,16]

Homopolymer-based PSCs have potential advantages over D−A alternating polymer-based systems because homopolymers have simpler structures of the single-type monomer, which produces shorter synthetic routes and reduces the time-cost for polymerization. However, despite these attractive features, almost no successful examples of homopolymers in high-performance PSCs have been reported, with the exception of poly(3-hexylthiophene) (P3HT). This is mainly due to their wide bandgap, nonoptimized energy levels, and steric hindrance by the adjacent repeating units that limit the values of short circuit current (J_{SC}) and open-circuit voltage (V_{OC}) in PSCs.[17] Although P3HT has been studied extensively as a polymer donor and has been demonstrated to provide PCE values in the range of 3−5% in PSCs, it has proven difficult to further improve their efficiency due to the higher-lying highest occupied molecular orbital (HOMO) energy level (−5.19 eV) and limited light absorption.[18−22] Therefore, in order to

Received: February 6, 2015
Revised: March 22, 2015
Published: March 23, 2015

DOI: 10.1021/acs.chemmater.5b00481
Chem. Mater. 2015, 27, 2653−2658

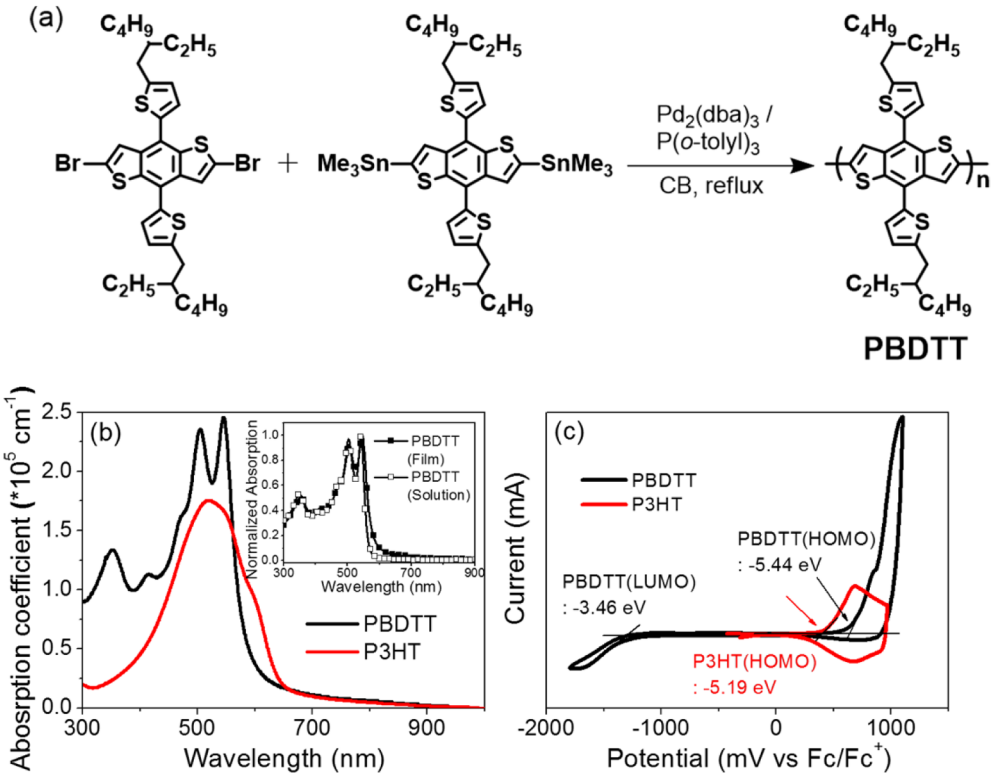

Figure 1. (a) Synthetic route for PBDTT; (b) absorption coefficients of PBDTT and P3HT films (inset: normalized UV−vis absorption spectra of PBDTT in dilute chloroform (□) and in film (■)); (c) cyclic voltammograms of PBDTT and P3HT films.

Table 1. Basic Properties of PBDTT Homopolymer

polymer	M_n/M_w (kg/mol)[a]	PDI (M_w/M_n)[a]	HOMO (eV)[b]	LUMO (eV)[b]	E_g^{cv} (eV)[b]	$E_g^{opt\ (sol)}$ (eV)[c]	$E_g^{opt\ (film)}$ (eV)[c]	T_d (°C)[d]
PBDTT	18.7/49.7	2.7	−5.44	−3.46	1.98	2.20	2.13	443

[a] M_n, M_w, and PDI were determined by SEC measurement using polystyrene standards in DCB at 80 °C. [b] Measured by CV. [c] Measured by UV−vis absorption spectroscopy. [d] Obtained from the TGA (5% weight loss temperature)

develop high-performance homopolymer-based PSCs, extensive effort is required to determine the appropriate molecular design of homopolymers. These efforts must be focused on (1) deep HOMO energy levels to increase the V_{OC} value and (2) high light-absorption coefficients and charge mobility to maximize the J_{SC} value by compensating for the lack of absorption in the long wavelengths and facilitating charge transport.

In this study, we designed and synthesized a homopolymer based on benzodithiophene (BDT) with a properly selected side chain via Stille coupling. We chose the BDT-based monomer, because BDT has a large planar conjugated structure and small steric hindrance between the adjacent repeating units.[17,23] Even though other groups have reported homopolymers based on BDT, their PCE values remained relatively low.[24−26] In this study, we developed the homopolymer based on thienyl-substituted benzodithiophene (BDTT) with branch-type side chains of 2-ethylhexyl to obtain deep HOMO energy level and to guarantee that the target polymer has high solubility. In addition, the two-dimensional, conjugated structure of the PBDTT can enhance the absorption coefficient, broaden the absorption band, and improve the thermal stability.[27,28] By fabricating the devices using a PBDTT:phenyl-C_{71}-butyric acid methyl ester ($PC_{71}BM$) (1:2, w/w) blend, we achieved the PCE value of 6.12%, which is the highest PCE value reported to date for homopolymer:PCBM-based PSCs.[24−26,29−34] Significantly, the optimized condition of the device was achieved without any solvent additive or thermal treatment. And, the PBDTT:$PC_{71}BM$ devices produced very high V_{OC} values approaching 1 V, demonstrating that PBDTT has great potential for use as a substitute for P3HT in PSCs with single and tandem device structure.

■ RESULTS AND DISCUSSION

The synthetic route of the PBDTT is shown in Figure 1a. The PBDTT was synthesized via Stille coupling between 2,6-dibromo-4,8-bis(5-(2-ethylhexyl)thiophen-2-yl)benzo[1,2-b:4,5-b']dithiophene (1 equiv) and (4,8-bis(5-(2-ethylhexyl)-thiophen-2-yl)benzo[1,2-b:4,5-b']dithiophene-2,6-diyl)bis-(trimethylstannane) (1 equiv) using $Pd_2(dba)_3$ (2 mol %) and P(*o*-tolyl)$_3$ (8 mol %) in chlorobenzene (CB) for 24 h. At the end of the polymerization, 2-bromothiophene (1 equiv) was added into the reactor, and then after 4 h, 2-tributylstannylthiophene (2 equiv) was sequentially added for an additional 4 h in order to improve the stability of the polymer by end-capping with thiophene.[35] After purification by Soxhlet extraction with methanol, acetone, hexane, dichloromethane, and chloroform, PBDTT was obtained by precipitating the chloroform fraction. The number-average molecular weight (M_n) and polydispersity index (PDI) of the PBDTT were 18.7 kg/mol and 2.66, respectively, as measured by size exclusion chromatography (SEC) with *o*-dichlorobenzene (DCB) as an eluent at 80 °C. The basic properties of the synthesized polymer are

DOI: 10.1021/acs.chemmater.5b00481
Chem. Mater. 2015, 27, 2653−2658

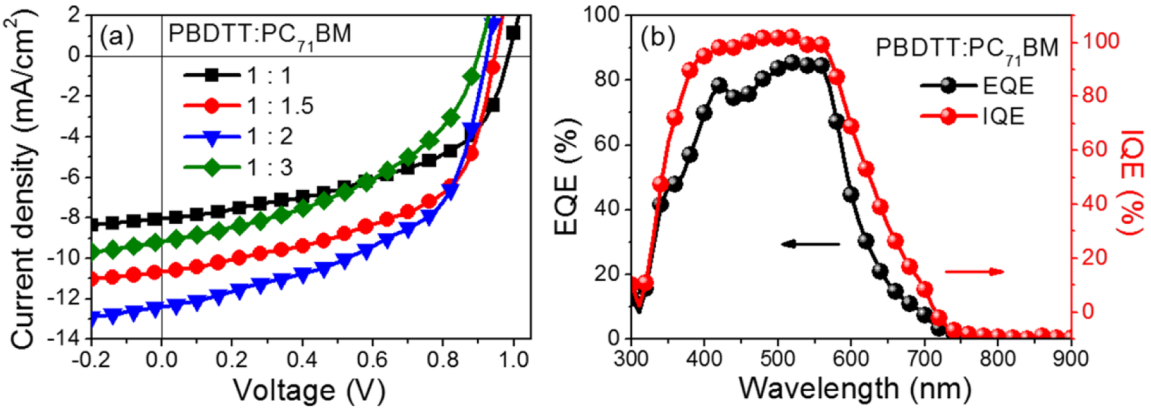

Figure 2. (a) Current−voltage (J−V) characteristics of BHJ-type PSCs based on PBDTT:$PC_{71}BM$ blend under AM 1.5 G illumination (100 mW/cm^2); (b) EQE and IQE values of the PSC at the optimized conditions.

Table 2. Photovoltaic Properties of the PBDTT:$PC_{71}BM$-Based PSCs (AM 1.5 G Illumination Conditions)

solvent	ratio[a]	V_{OC} (V)	J_{SC} (mA cm^{-2})	FF	PCE_{max} (PCE_{ave})[b](%)	Cal. J_{SC} (mA cm^{-2})[c]	thickness (nm)
DCB	1:1	1.00	8.01	0.49	3.92 (3.86)	7.73	75
	1:1.5	0.96	10.64	0.53	5.41 (5.25)	10.26	85
	1:2	0.93	11.95	0.55	6.12 (6.06)	11.47	95
	1:3	0.90	9.15	0.44	3.63 (3.56)	8.75	110
+1% DIO	1:2	0.90	11.20	0.53	5.39 (5.31)	10.92	90
+1% DPE	1:2	0.94	11.83	0.50	5.57 (5.40)	11.45	95

[a]PBDTT:$PC_{71}BM$ weight ratio [b]The average PCE values were obtained from more than 10 separate devices [c]Calculated J_{SC} values from EQE.

summarized in Table 1. The synthesized polymer structure was characterized by proton nuclear magnetic resonance (^1H NMR) (see Figure S1 in the Supporting Information). Thermogravimetric analysis (TGA) measurement was employed to evaluate the thermal stability of the polymer. It was observed that the decomposition temperature (T_d) of PBDTT at 5% weight loss was 443 °C, which is a significantly higher value than those of many other BDT-based D−A alternating polymers (Figure S2 in the Supporting Information),[1,5,27,36−39] and differential scanning calorimetry results showed no thermal transition from 20 to 300 °C.

The optical and electrochemical properties of the conjugated polymers are important for determining their performance in PSCs. Figure 1b shows the optical properties of PBDTT in dilute chloroform solution and thin film. The spectrum of PBDTT in the thin film shows three absorption peaks, including a distinct absorption peak at 506 nm ascribed to the π−π^* transition between BDT, and a peak at 546 nm attributed to the vibronic peak. The absorption in solution is almost the same as that of the thin film, implying that a certain degree of packing structure is formed in solution. On the basis of the onset of the light absorption in the thin film, the optical bandgap of PBDTT is 2.13 eV. Interestingly, the absorption coefficient of PBDTT is 2.5×10^5 cm^{-1}, which is approximately 40% higher value than that of P3HT (1.8×10^5 cm^{-1}), indicating that the PBDTT film can absorb sunlight more efficiently than the P3HT film with the same thickness (Figure 1b). The HOMO and lowest unoccupied molecular orbital (LUMO) energy levels of PBDTT were determined by cyclic voltammetry (CV) measurement (Figure 1c). The HOMO and LUMO energy levels of PBDTT were estimated to be −5.44 and −3.46 eV from the onset oxidation potentials (E_{onset}^{ox}) and the onset reduction potentials (E_{onset}^{red}), respectively. In the case of P3HT, the LUMO energy level (−3.27 eV) was much higher than that of $PC_{71}BM$ (−3.85 eV), thereby inducing a large loss of LUMO−LUMO offset and then decreasing V_{OC}.[19,40] In contrast, PBDTT has a deep HOMO energy level lower than that of P3HT by 0.2 eV, whereas sufficient LUMO−LUMO offset is still guaranteed for efficient exciton dissociation with $PC_{71}BM$. Therefore, the PBDTT-based devices can be expected to yield higher V_{OC} values than P3HT-based devices, because the V_{OC} is linearly proportional to the difference in energy between the HOMO of the electron donor and the LUMO of the electron acceptor.[41,42]

To explore the potential of PBDTT in the PSCs, BHJ-type PSCs were fabricated with a conventional device structure of indium tin oxide (ITO)/poly(3,4-ethylenedioxythiophene):poly(styrenesulfonate) (PEDOT:PSS)/PBDTT:$PC_{71}BM$/LiF/Al, and their performances were measured using an AM 1.5 solar simulator (Figure 2a and Figure S3 in the Supporting Information). $PC_{71}BM$ was chosen as the electron acceptor instead of $PC_{61}BM$ because it absorbs more light in the visible range.[43] Several devices with different weight ratios of PBDTT:$PC_{71}BM$ ranging from 1:1 to 1:3 in DCB were investigated without the use of solvent additive. The J_{SC} values of the devices increased from 8.01 mA cm^{-2} at a 1:1 blend ratio to 10.64 mA cm^{-2} at a 1:1.5 blend ratio, to 11.95 mA cm^{-2} at a 1:2 blend ratio, and then decreased to 9.15 mA cm^{-2} at a 1:3 blend ratio (Table 2). In particular, remarkably high V_{OC} value of up to 1.00 V was obtained for PBDTT:$PC_{71}BM$ (1:1, w/w), which should benefit from the deep HOMO energy level of PBDTT. To the best of our knowledge, this is one of the highest V_{OC} values reported to date for high-performance homopolymer:PCBM-based BHJ-type PSCs.[24−26,29−34] However, the V_{OC} values decreased slightly as the content of $PC_{71}BM$ increased due to a reduction in the charge transfer energy.[44,45] At the 1:2 blend ratio of PBDTT:$PC_{71}BM$, the best device performance of 6.12% was achieved with V_{OC} of 0.93 V, J_{SC} of 11.95 mA cm^{-2}, and FF of 0.55. This PCE value is significantly higher than that of

DOI: 10.1021/acs.chemmater.5b00481
Chem. Mater. 2015, 27, 2653−2658

P3HT:PCBM for the conventional device structure.[46−48] To examine opportunities for further enhancing the device performance, we applied various types of solvent additives, including DIO and diphenyl ether (DPE), to the blend of PBDTT:$PC_{71}BM$ (1:2, w/w), but none of the additional processing increased the efficiency of the PBDTT:$PC_{71}BM$ PSCs.[12,49−51] Thus, the best PCE of PBDTT:$PC_{71}BM$ was achieved without any additive or thermal treatment.

Figure 2b shows the external quantum efficiency (EQE) and internal quantum efficiency (IQE) curves of PBDTT:$PC_{71}BM$ (1:2, w/w) for the optimized conditions. The EQE curves of the PBDTT:$PC_{71}BM$ devices with different blend weight ratios are also shown in Figure S4 in the Supporting Information. The EQE spectra were observed in the range of 350−650 nm, which is consistent with the UV−vis absorption range for the blend film (Figure S5 in the Supporting Information). The PBDTT:$PC_{71}BM$ device (1:2, w/w) showed efficient photoconversion efficiencies exceeding 75% in the range of 380−560 nm with the maximum EQE value of 85% at 520 nm, which is a remarkably high EQE value for PSCs. The measured J_{SC} values of the PBDTT:$PC_{71}BM$ blends were well matched with the integrated values obtained from their EQE spectra within an error of 4%. In addition, the IQE values were calculated by dividing the EQE values by the fraction of photons absorbed in the active layer (Figure 2b).[52,53] The IQE spectrum exhibited a high value of more than 90% in a wide range from 400 to 560 nm, with the maximum IQE value of 93% occurring at 510 nm. Such a high IQE in this system implies that the active layer is close to ideal morphology, thereby providing efficient exciton diffusion, charge separation, and carrier collection to each electrode, and facilitating the most absorbed photons converted into photocurrent. The high IQE values of the PBDTT:$PC_{71}BM$ device can be supported by well-balanced hole and electron mobilities measured by the space charge limited current (SCLC) method (Figure S6 in the Supporting Information). The hole and electron motilities of the PBDTT:$PC_{71}BM$ blend were 5.84×10^{-5} and 1.04×10^{-4} $cm^2\ V^{-1}\ s^{-1}$, respectively, indicating that the balanced transport of holes and electrons in the PBDTT:$PC_{71}BM$ device reduced the charge recombination.[54,55]

To gain insight into the operation of the BHJ solar cells, we investigated the morphology of PBDTT:$PC_{71}BM$ blend by grazing incidence X-ray scattering (GIXS), resonant soft X-ray scattering (RSoXS), and tapping-mode atomic force microscopy (AFM). First, GIXS measurements were used to investigate the molecular packing of pristine PBDTT and PBDTT:$PC_{71}BM$ blend films under optimized device conditions (Figure 3a). The in-plane X-ray profile (Figure S7a in the Supporting Information) indicates that the pristine PBDTT exhibited (100) diffraction peak at q = 0.28 $Å^{-1}$, which corresponds to the lamellar spacing of 22.4 Å. The pristine PBDTT exhibited a distinctive arc scattering of the (010) peak along the out-of-plane direction at q = 1.76 $Å^{-1}$, which corresponds to $\pi-\pi$ stacking distance of 3.55 Å. Thus, the PBDTT exhibited a smaller $\pi-\pi$ stacking distance compared to those of P3HT and most of BDT-based alternating copolymers,[56−61] which indicates the formation of tighter interchain packing that should increase electron mobility.[62] In addition, the $\pi-\pi$ stacking peak was prominent in the out-of-plane direction, suggesting that most of the polymer backbones were face-on oriented relative to the substrates. Moreover, the orientation and distance of the $\pi-\pi$ stacking of the PBDTT were well-preserved even after the addition of $PC_{71}BM$, which

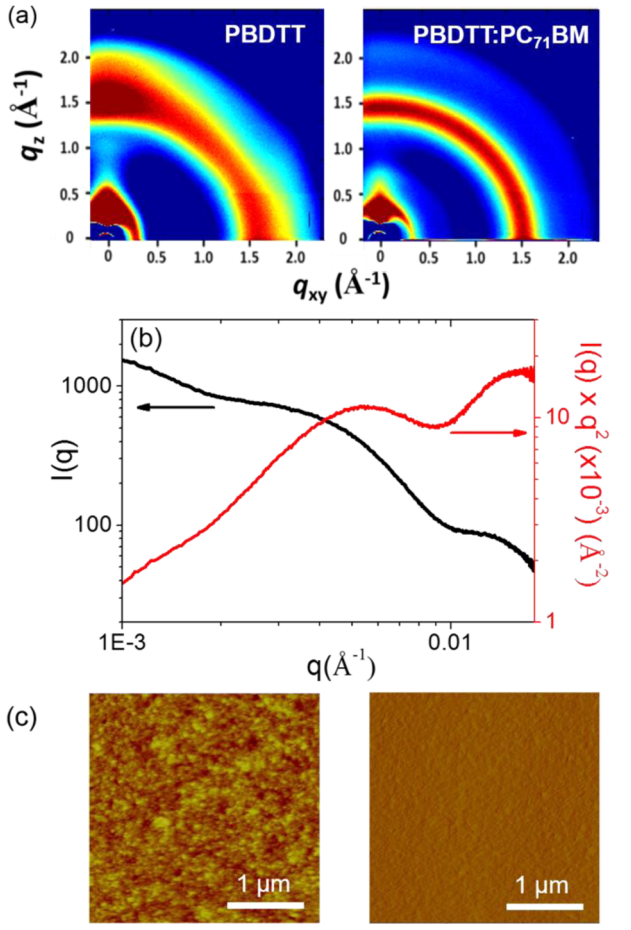

Figure 3. (a) GIXS patterns of pristine PBDTT and PBDTT:$PC_{71}BM$ blend films under the optimized device condition; (b) RSoXS profiles of PBDTT:$PC_{71}BM$ blend film under the optimized device condition at 280 eV; (c) AFM height (left) and phase (right) images of the PBDTT:$PC_{71}BM$ blend film (the scale bar is 1 μm).

was beneficial for efficient charge transport in the blend device.[60,63]

The BHJ morphology of the PBDTT:$PC_{71}BM$ blend film (1:2, w/w) under the optimized device condition was probed by RSoXS technique (Figure 3b and Figure S8 in the Supporting Information), which can provide precise information about the degree of macroscopic phase separation.[64−66] The RSoXS data were obtained using a series of photon energies to observe the scattering in the range of the tens to hundreds of nanometers. Figure 3b shows a plot of the intensity ($I(q)$) vs q at 280 eV. In addition, the intensity was multiplied by q^2 for better recognition of the relative intensities in the low q regime. Interestingly, the PBDTT:$PC_{71}BM$ blend had bimodal peaks at the maximum values at q = 0.005 and q = 0.015 $Å^{-1}$, respectively, corresponding to the domain spacing lengths ($d = 2\pi/q$) of 125 and 42 nm. It is suggested on the basis of the observation with multiple photon energies that the two scattering peaks were not from the form factor. In addition, both peaks were quite broad, indicating that their size distribution of phase-separated domains should be very broad. Such phase separation with a multiple-length scale was considered to be beneficial for facilitating charge separation and transport, which also has been observed in other PSC systems.[67,68] We noted that the multiple-length scale phase separation was observed for the PBDTT:$PC_{71}BM$ blend

DOI: 10.1021/acs.chemmater.5b00481
Chem. Mater. 2015, 27, 2653−2658

without any solvent additive treatment, whereas the solvent additives serve an important role in producing such phase separation in other systems based on the D−A alternating polymers. We speculate that the homogeneity of PBDTT with highly planar BDTT units can promote their interchain interactions and assembly. In addition, the AFM images confirmed that the PBDTT:$PC_{71}BM$ blend had a well-mixed, interpenetrating network and small-scale phase separation separation with the root-mean-square (RMS) surface roughness of 0.81 ± 0.02 nm. (Figure 3c). These results were in good agreement with the RSoXS results, which supported the high EQE and IQE values of our PBDTT:$PC_{71}BM$-based PSC.

The thermal stability of the PBDTT:$PC_{71}BM$-based devices with and without additive (DIO) was examined because the thermally stable operation of the PSCs is of great importance for their commercial application. In this regard, the performance of PBDTT:$PC_{71}BM$ devices with a structure of ITO/PEDOT:PSS/active layer/Al was monitored as a function of time at 90 °C under a nitrogen atmosphere (Figure 4). The

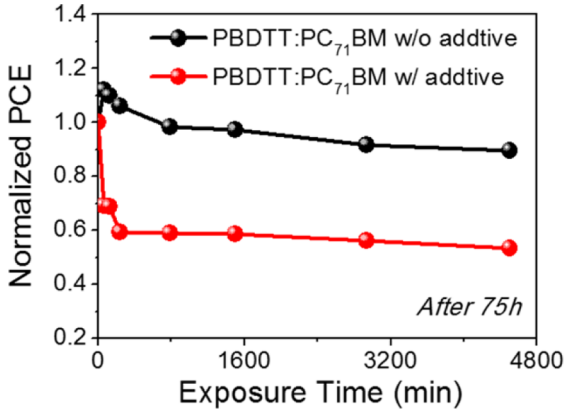

Figure 4. Normalized PCE values of PBDTT:$PC_{71}BM$ devices with and without additive measured for different annealing times at 90 °C.

buffer electrode, LiF, was excluded to elucidate the correlation between the polymer structure and the thermal stability of their PSCs, because the PCE values of the devices are strongly affected by the diffusion of LiF during thermal annealing.[69] After thermal annealing for 75 h at 90 °C, the device performance with and without additive showed a stark difference in their tendencies to change the PCE, i.e., the PCE value of the PBDTT:$PC_{71}BM$ device without additive was decreased by only 10%, whereas the PCE value of the device with additive was dramatically reduced by 54%, suggesting that the additive-free system is essential to increase the morphological stability. Therefore, the PBDTT-based PSCs have the potential advantages of additive-free fabrication and long-term thermal stability.

CONCLUSION

PBDTT homopolymer was easily synthesized via Stille coupling for the electron donor material in the PSCs. The PBDTT had lower HOMO energy level (−5.44 eV) and higher absorption coefficient (2.5×10^5 cm^{-1}) than P3HT, thereby exhibiting the PCE value of 6.12% with high V_{OC} of 0.93 V. High J_{SC} and IQE values (above 93%) were obtained due to the well-optimized BHJ morphology that had finely phase-separated domains with bimodal-scale lengths. Therefore, the PBDTT has great potential for use as a novel polymer donor to replace P3HT as the wide band gap polymer in tandem solar cells and ternary blend solar cells. Also, we demonstrated that the optimization of the PBDTT:$PC_{71}BM$ device was obtained without any solvent additive or thermal treatment, which makes PBDTT promising candidate as polymer donor for flexible, large-area PSCs.

ASSOCIATED CONTENT

Supporting Information

Materials and characterization methods, detail experimental procedures, and additional data. This material is available free of charge via the Internet at http://pubs.acs.org.

AUTHOR INFORMATION

Corresponding Author

*E-mail: bumjoonkim@kaist.ac.kr.

Notes

The authors declare no competing financial interest.

ACKNOWLEDGMENTS

This research was supported by the Global Frontier R&D Program on Center for Multiscale Energy System (2012M3A6A7055540), funded by the Korean Government. This research was supported by the New & Renewable Energy Program of KETEP Grant (20133030000130, 20133030011330), funded by the Ministry of Trade, industry & Energy, Republic of Korea. This research was also supported by the Research Projects of the KAIST-KUSTAR and the CRH(Climate Change Research Hub) of KAIST.

REFERENCES

(1) Zhang, S.; Ye, L.; Zhao, W.; Liu, D.; Yao, H.; Hou, J. *Macromolecules* **2014**, *47*, 4653−4659.
(2) Cabanetos, C.; El Labban, A.; Bartelt, J. A.; Douglas, J. D.; Mateker, W. R.; Frechet, J. M. J.; McGehee, M. D.; Beaujuge, P. M. *J. Am. Chem. Soc.* **2013**, *135*, 4656−4659.
(3) Dou, L. T.; Chang, W. H.; Gao, J.; Chen, C. C.; You, J. B.; Yang, Y. *Adv. Mater.* **2013**, *25*, 825−831.
(4) Liang, Y. Y.; Xu, Z.; Xia, J. B.; Tsai, S. T.; Wu, Y.; Li, G.; Ray, C.; Yu, L. P. *Adv. Mater.* **2010**, *22*, E135−E138.
(5) Dou, L. T.; Gao, J.; Richard, E.; You, J. B.; Chen, C. C.; Cha, K. C.; He, Y. J.; Li, G.; Yang, Y. *J. Am. Chem. Soc.* **2012**, *134*, 10071−10079.
(6) Li, Y. F. *Acc. Chem. Res.* **2012**, *45*, 723−733.
(7) Son, H. J.; Carsten, B.; Jung, I. H.; Yu, L. P. *Energy Environ. Sci.* **2012**, *5*, 8158−8170.
(8) Zhang, Z. G.; Wang, J. Z. *J. Mater. Chem.* **2012**, *22*, 4178−4187.
(9) Shrotriya, V. *Nat. Photonics* **2009**, *3*, 447−449.
(10) Krebs, F. C.; Jørgensen, M.; Norrman, K.; Hagemann, O.; Alstrup, J.; Nielsen, T. D.; Fyenbo, J.; Larsen, K.; Kristensen, J. *Sol. Energy Mater. Sol. Cells* **2009**, *93*, 422−441.
(11) Zhang, M. J.; Gu, Y.; Guo, X.; Liu, F.; Zhang, S. Q.; Huo, L. J.; Russell, T. P.; Hou, J. H. *Adv. Mater.* **2013**, *25*, 4944−4949.
(12) Lee, J. K.; Ma, W. L.; Brabec, C. J.; Yuen, J.; Moon, J. S.; Kim, J. Y.; Lee, K.; Bazan, G. C.; Heeger, A. J. *J. Am. Chem. Soc.* **2008**, *130*, 3619−3623.
(13) Wang, E. G.; Ma, Z. F.; Zhang, Z.; Vandewal, K.; Henriksson, P.; Inganas, O.; Zhang, F. L.; Andersson, M. R. *J. Am. Chem. Soc.* **2011**, *133*, 14244−14247.
(14) Ye, L.; Zhang, S. Q.; Ma, W.; Fan, B. H.; Guo, X.; Huang, Y.; Ade, H.; Hou, J. H. *Adv. Mater.* **2012**, *24*, 6335−6341.
(15) Chang, L. L.; Lademann, H. W. A.; Bonekamp, J. B.; Meerholz, K.; Moule, A. J. *Adv. Funct. Mater.* **2011**, *21*, 1779−1787.
(16) Ye, L.; Jing, Y.; Guo, X.; Sun, H.; Zhang, S. Q.; Zhang, M. J.; Huo, L. J.; Hou, J. H. *J. Phys. Chem. C* **2013**, *117*, 14920−14928.

DOI: 10.1021/acs.chemmater.5b00481
Chem. Mater. 2015, 27, 2653−2658

(17) Zhou, H. X.; Yang, L. Q.; You, W. *Macromolecules* **2012**, *45*, 607−632.
(18) Kim, Y.; Cook, S.; Tuladhar, S. M.; Choulis, S. A.; Nelson, J.; Durrant, J. R.; Bradley, D. D. C.; Giles, M.; Mcculloch, I.; Ha, C. S.; Ree, M. *Nat. Mater.* **2006**, *5*, 197−203.
(19) Kang, H.; Cho, C. H.; Cho, H. H.; Kang, T. E.; Kim, H. J.; Kim, K. H.; Yoon, S. C.; Kim, B. J. *ACS Appl. Mater. Interfaces* **2012**, *4*, 110−116.
(20) Ma, W. L.; Yang, C. Y.; Gong, X.; Lee, K.; Heeger, A. J. *Adv. Funct. Mater.* **2005**, *15*, 1617−1622.
(21) Lenes, M.; Wetzelaer, G. J. A. H.; Kooistra, F. B.; Veenstra, S. C.; Hummelen, J. C.; Blom, P. W. M. *Adv. Mater.* **2008**, *20*, 2116−2119.
(22) Dang, M. T.; Hirsch, L.; Wantz, G. *Adv. Mater.* **2011**, *23*, 3597−3602.
(23) Hou, J. H.; Park, M. H.; Zhang, S. Q.; Yao, Y.; Chen, L. M.; Li, J. H.; Yang, Y. *Macromolecules* **2008**, *41*, 6012−6018.
(24) Lee, D.; Hubijar, E.; Kalaw, G. J. D.; Ferraris, J. P. *Chem. Mater.* **2012**, *24*, 2534−2540.
(25) Magurudeniya, H. D.; Kularatne, R. S.; Rainbolt, E. A.; Bhatt, M. P.; Murphy, J. W.; Sheina, E. E.; Gnade, B. E.; Biewer, M. C.; Stefan, M. C. *Journal of Materials Chemistry A* **2014**, *2*, 8773−8781.
(26) Sista, P.; Xue, B. F.; Wilson, M.; Holmes, N.; Kularatne, R. S.; Nguyen, H.; Dastoor, P. C.; Belcher, W.; Poole, K.; Janesko, B. G.; Biewer, M. C.; Stefan, M. C. *Macromolecules* **2012**, *45*, 772−780.
(27) Huo, L. J.; Zhang, S. Q.; Guo, X.; Xu, F.; Li, Y. F.; Hou, J. H. *Angew. Chem., Int. Ed.* **2011**, *123*, 9871−9876.
(28) Duan, R. M.; Ye, L.; Guo, X.; Huang, Y.; Wang, P.; Zhang, S. Q.; Zhang, J. P.; Huo, L. J.; Hou, J. H. *Macromolecules* **2012**, *45*, 3032−3038.
(29) Cho, C. H.; Kim, H. J.; Kang, H.; Shin, T. J.; Kim, B. J. *J. Mater. Chem.* **2012**, *22*, 14236−14245.
(30) Zhou, H. X.; Yang, L. Q.; Stoneking, S.; You, W. *ACS Appl. Mater. Interfaces* **2010**, *2*, 1377−1383.
(31) Cho, C. H.; Kang, H.; Kang, T. E.; Cho, H. H.; Yoon, S. C.; Jeon, M. K.; Kim, B. J. *Chem. Commun.* **2011**, *47*, 3577−3579.
(32) Xiao, S. Q.; Stuart, A. C.; Liu, S. B.; Zhou, H. X.; You, W. *Adv. Funct. Mater.* **2010**, *20*, 635−643.
(33) Burkhart, B.; Khlyabich, P. P.; Thompson, B. C. *Macromolecules* **2012**, *45*, 3740−3748.
(34) Ren, G. Q.; Wu, P. T.; Jenekhe, S. A. *Chem. Mater.* **2010**, *22*, 2020−2026.
(35) Park, J. K.; Jo, J.; Seo, J. H.; Moon, J. S.; Park, Y. D.; Lee, K.; Heeger, A. J.; Bazan, G. C. *Adv. Mater.* **2011**, *23*, 2430−2435.
(36) Cho, H. H.; Kang, T. E.; Kim, K. H.; Kang, H.; Kim, H. J.; Kim, B. J. *Macromolecules* **2012**, *45*, 6415−6423.
(37) Chen, H. C.; Chen, Y. H.; Liu, C. C.; Chien, Y. C.; Chou, S. W.; Chou, P. T. *Chem. Mater.* **2012**, *24*, 4766−4772.
(38) Huo, L. J.; Guo, X.; Zhang, S. Q.; Li, Y. F.; Hou, J. H. *Macromolecules* **2011**, *44*, 4035−4037.
(39) Peng, Q.; Liu, X. J.; Su, D.; Fu, G. W.; Xu, J.; Dai, L. M. *Adv. Mater.* **2011**, *23*, 4554−4558.
(40) Veldman, D.; Meskers, S. C. J.; Janssen, R. A. J. *Adv. Funct. Mater.* **2009**, *19*, 1939−1948.
(41) Brabec, C. J.; Cravino, A.; Meissner, D.; Sariciftci, N. S.; Fromherz, T.; Rispens, M. T.; Sanchez, L.; Hummelen, J. C. *Adv. Funct. Mater.* **2001**, *11*, 374−380.
(42) Kim, K. H.; Kang, H.; Nam, S. Y.; Jung, J.; Kim, P. S.; Cho, C. H.; Lee, C.; Yoon, S. C.; Kim, B. J. *Chem. Mater.* **2011**, *23*, 5090−5095.
(43) Wienk, M. M.; Kroon, J. M.; Verhees, W. J. H.; Knol, J.; Hummelen, J. C.; van Hal, P. A.; Janssen, R. A. J. *Angew. Chem., Int. Ed.* **2003**, *42*, 3371−3375.
(44) Vandewal, K.; Gadisa, A.; Oosterbaan, W. D.; Bertho, S.; Banishoeib, F.; Van Severen, I.; Lutsen, L.; Cleij, T. J.; Vanderzande, D.; Manca, J. V. *Adv. Funct. Mater.* **2008**, *18*, 2064−2070.
(45) Piersimoni, F.; Chambon, S.; Vandewal, K.; Mens, R.; Boonen, T.; Gadisa, A.; Izquierdo, M.; Filippone, S.; Ruttens, B.; D'Haen, J.; Martin, N.; Lutsen, L.; Vanderzande, D.; Adriaensens, P.; Manca, J. V. *J. Phys. Chem. C* **2011**, *115*, 10873−10880.
(46) Wang, D. H.; Kim, J. K.; Lim, G. H.; Park, K. H.; Park, O. O.; Lim, B.; Park, J. H. *RSC Advances* **2012**, *2*, 7268−7272.
(47) Kim, J. Y.; Noh, S.; Nam, Y. M.; Kim, J. Y.; Roh, J.; Park, M.; Amsden, J. J.; Yoon, D. Y.; Lee, C.; Jo, W. H. *ACS Appl. Mater. Interfaces* **2011**, *3*, 4279−4285.
(48) Chen, S. F.; Cheng, F.; Mei, Y.; Peng, B.; Kong, M.; Hao, J. Y.; Zhang, R.; Xiong, Q. H.; Wang, L. H.; Huang, W. *Appl. Phys. Lett.* **2014**, *104*, 213903.
(49) Lou, S. J.; Szarko, J. M.; Xu, T.; Yu, L. P.; Marks, T. J.; Chen, L. X. *J. Am. Chem. Soc.* **2011**, *133*, 20661−20663.
(50) Su, M. S.; Kuo, C. Y.; Yuan, M. C.; Jeng, U. S.; Su, C. J.; Wei, K. H. *Adv. Mater.* **2011**, *23*, 3315−3319.
(51) Etzold, F.; Howard, I. A.; Forler, N.; Cho, D. M.; Meister, M.; Mangold, H.; Shu, J.; Hansen, M. R.; Mullen, K.; Laquai, F. *J. Am. Chem. Soc.* **2012**, *134*, 10569−10583.
(52) Baek, S. W.; Noh, J.; Lee, C. H.; Kim, B.; Seo, M. K.; Lee, J. Y. *Sci. Rep.* **2013**, *3*, 1726−1732.
(53) Kim, T.; Kang, H.; Jeong, S.; Kang, D. J.; Lee, C.; Lee, C. H.; Seo, M. K.; Lee, J. Y.; Kim, B. J. *ACS Appl. Mater. Interfaces* **2014**, *6*, 16956−16965.
(54) Chen, M. C.; Liaw, D. J.; Chen, W. H.; Huang, Y. C.; Sharma, J.; Tai, Y. *Appl. Phys. Lett.* **2011**, *99*, 223305−223307.
(55) Chang, Y. T.; Hsu, S. L.; Su, M. H.; Wei, K. H. *Adv. Mater.* **2009**, *21*, 2093−2097.
(56) Kim, H. J.; Han, A. R.; Cho, C. H.; Kang, H.; Cho, H. H.; Lee, M. Y.; Frechet, J. M. J.; Oh, J. H.; Kim, B. J. *Chem. Mater.* **2012**, *24*, 215−221.
(57) Kim, B. J.; Miyamoto, Y.; Ma, B. W.; Frechet, J. M. J. *Adv. Funct. Mater.* **2009**, *19*, 2273−2281.
(58) Kang, T. E.; Cho, H.-H.; Kim, H. j.; Lee, W.; Kang, H.; Kim, B. J. *Macromolecules* **2013**, *46*, 6806−6813.
(59) Gao, J.; Dou, L. T.; Chen, W.; Chen, C. C.; Guo, X. R.; You, J. B.; Bob, B.; Chang, W. H.; Strzalka, J.; Wang, C.; Li, G.; Yang, Y. *Adv. Energy Mater.* **2014**, *4*, 1300739−1300746.
(60) Piliego, C.; Holcombe, T. W.; Douglas, J. D.; Woo, C. H.; Beaujuge, P. M.; Frechet, J. M. J. *J. Am. Chem. Soc.* **2010**, *132*, 7595−7597.
(61) He, X. X.; Mukherjee, S.; Watkins, S.; Chen, M.; Qin, T. S.; Thomsen, L.; Ade, H.; McNeill, C. R. *J. Phys. Chem. C* **2014**, *118*, 9918−9929.
(62) Steyrleuthner, R.; Di Pietro, R.; Collins, B. A.; Polzer, F.; Himmelberger, S.; Schubert, M.; Chen, Z.; Zhang, S.; Salleo, A.; Ade, H. *J. Am. Chem. Soc.* **2014**, *136*, 4245−4256.
(63) Beaujuge, P. M.; Frechet, J. M. J. *J. Am. Chem. Soc.* **2011**, *133*, 20009−20029.
(64) Yan, H.; Collins, B. A.; Gann, E.; Wang, C.; Ade, H.; McNeill, C. R. *ACS Nano* **2011**, *6*, 677−688.
(65) Swaraj, S.; Wang, C.; Yan, H.; Watts, B.; Lüning, J.; McNeill, C. R.; Ade, H. *Nano Lett.* **2010**, *10*, 2863−2869..
(66) Chen, D.; Liu, F.; Wang, C.; Nakahara, A.; Russell, T. P. *Nano Lett.* **2011**, *11*, 2071−2078.
(67) Gu, Y.; Wang, C.; Russell, T. P. *Adv. Energy Mater.* **2012**, *2*, 683−690.
(68) Chen, W.; Xu, T.; He, F.; Wang, W.; Wang, C.; Strzalka, J.; Liu, Y.; Wen, J.; Miller, D. J.; Chen, J. *Nano Lett.* **2011**, *11*, 3707−3713.
(69) Mateker, W. R.; Douglas, J. D.; Cabanetos, C.; Sachs-Quintana, I. T.; Bartelt, J. A.; Hoke, E. T.; El Labban, A.; Beaujuge, P. M.; Frechet, J. M. J.; McGehee, M. D. *Energy Environ. Sci.* **2013**, *6*, 2529−2537.

DOI: 10.1021/acs.chemmater.5b00481
Chem. Mater. 2015, 27, 2653−2658